Journal of Power Sources 330 (2016) 186–194

Contents lists available at ScienceDirect

Journal of Power Sources

journal homepage: www.elsevier.com/locate/jpowsour

Graphite electrode thermal behavior and solid electrolyte interphase investigations: Role of state-of-the-art binders, carbonate additives and lithium bis(fluorosulfonyl)imide salt

Coralie Forestier [a, b, c, d], Sylvie Grugeon [a, b], Carine Davoisne [a, b], Amandine Lecocq [c], Guy Marlair [c], Michel Armand [a], Lucas Sannier [d], Stephane Laruelle [a, b, *]

[a] Laboratoire de Réactivité et Chimie des Solides, CNRS UMR 7314, Université de Picardie Jules Verne, 33 rue Saint Leu, 80039 Amiens, France
[b] Réseau sur le Stockage Electrochimique de l'Energie, CNRS RS2E FR3459, France
[c] Institut National de l'Environnement Industriel et des Risques (INERIS), Parc Technologique Alata, BP2, 60550 Verneuil-en-Halatte, France
[d] Renault, DEA-IREB, Renault Technocentre, 1 avenue du Golf, 78288 Guyancourt, France

HIGHLIGHTS

- Lower and better distributed heat energy released with SBR/CMC binders.
- SBR is involved in the thermal processes.
- The polymeric nature of the VC-derived SEI is preferable for safer batteries.
- The 0.33 M LiFSI and 0.66 M $LiPF_6$ salt ratio hinders Al corrosion up to 4.3 V
- The 0.33 M LiFSI and 0.66 M $LiPF_6$ salt ratio improves the thermal behavior.

ARTICLE INFO

Article history:
Received 7 May 2016
Received in revised form
12 July 2016
Accepted 2 September 2016
Available online 10 September 2016

Keywords:
SEI
DSC
Thermal runaway
LiFSI
VC
FEC

ABSTRACT

The risk of thermal runaway is, for Li-ion batteries, a critical issue for large-scale applications. This results in manufacturers and researchers placing great emphasis on minimizing the heat generation and thereby mitigating safety-related risks through the search for suitable materials or additives. To this end, an in-depth stepwise investigation has been undertaken to provide a better understanding of the exothermic processes that take place at the negative electrode/electrolyte interface as well as an increased visibility of the role of the state-of-the-art electrode binders, additives and lithium salt by means of the classical DSC technique.

A reliable experimental set up helped quantify the beneficial or harmful contribution of binder polymers to the exothermic behavior of the CMC/SBR containing graphite electrode film in contact with 1 M $LiPF_6$ in EC:DMC:EMC (1:1:1 v/v/v) electrolyte.

Further, the role of the VC, FEC and VEC electrolyte additives (2 wt%) in reinforcing the protective SEI layer towards thermally induced electrolyte reduction is discussed in the light of infrared spectroscopy and transmission electron microscopy analyzes results.

Moreover, after a preliminary corrosion study of $LiPF_6$/LiFSI mixtures, we showed that the 0.66/0.33 M composition can be used in commercial NMC-based LiBs with a positive effect on the thermal runaway.

© 2016 Elsevier B.V. All rights reserved.

1. Introduction

The development of greener transportation is an alternative to mitigate environmental concerns and energy dependence on fossil fuels. Due to their high energy density and long cycle life, Li-ion batteries (LiBs) are the most attractive power source for electrical vehicles (EV) and hybrid electric vehicles (HEV). However, the use

* Corresponding author. Laboratoire de Réactivité et Chimie des Solides, CNRS UMR 7314, Université de Picardie Jules Verne, 33 rue Saint Leu, 80039 Amiens, France.
E-mail address: stephane.laruelle@u-picardie.fr (S. Laruelle).

http://dx.doi.org/10.1016/j.jpowsour.2016.09.005
0378-7753/© 2016 Elsevier B.V. All rights reserved.

of high energy LiBs imposes stringent safety requirements either to comply with international transport regulations or with regard to end use, though standardized safety tests are described in technical documents from various sources [1] (UL, ANSI, SEA, ISO, IEC and US ABC). These tests are widely performed at different scales (cell, battery, pack), and they are sometimes amended according to technical and scientific progress in order to ever more adequately reflect a battery failure process. Calorimetry techniques (DSC, ARC) are the techniques of choice for appraising thermal behaviors at component and cell levels respectively and coupling them with analytical methods [2–7] (FTIR, XRD, GC-MS, XPS …) can help identify the mechanisms involved during abusive use conditions.

The internal temperature rise can lead to thermal runaway triggered by several exothermic phenomena stemming from reduction/oxidation of the electrolyte as well as thermal decomposition of battery components (electrolyte [8–12], anode [3–5,7,13–20], cathode [21–24] and separator [25,26]) up to partial or complete oxidation of these components according to effective adverse effects of the thermal runaway process. As the first exothermic reaction takes place at the negative electrode/electrolyte interface, improving the understanding of the thermal behavior of this interface and more accurately assessing the safety gains (higher onset temperature of exothermic reactions, less related energy release) associated with an electrolyte or composite compound change is of utmost interest. Over the past two decades, a plethora of studies have been devoted to the elucidation of some of the cascade reactions involved in the thermal runaway complex phenomenon. The most important one relates to the SEI breakdown. Starting from 100 °C, the basic salts [27,28] (lithium carbonate Li_2CO_3, lithium alkyl carbonates $ROCO_2Li$, $(CH_2OCO_2Li)_2$) from the passivating layer (Solid Electrolyte Interphase -SEI- [29]) issuing from the carbonate solvents electrochemical reduction first react with gaseous PF_5 [17], coming from $LiPF_6$ salt thermal degradation [10,30–34]. These acid-base reactions promoted by the high volatility of linear carbonates in turn damage the SEI, hence facilitating the access of the electrolyte to the lithiated graphite. Such a consensual assumption offers a promising outlook to shift the SEI decomposition to higher temperature by changing its composition and limiting PF_5 formation.

Commercial electrolytes essentially consist in various binary or ternary mixtures of carbonate-based solvents (EC, PC, DMC, DEC, DMC) with $LiPF_6$ salt. Electrolyte additives (<10%) are added, in particular to improve the physical properties of the SEI during the formation of the LIBs and, consequently, to enhance their cyclability. The most popular additives enhancing SEI properties are i) vinylene carbonate (VC), ii) fluoroethylene carbonate (FEC) and iii) vinyl ethylene carbonate (VEC). On a safety point of view, the addition of VC leads to a higher onset temperature and a decrease of the total heat release upon heating of lithiated graphite [35]. FEC, which is widely used in the case of silicon electrodes, is reported to also improve the thermal stability of lithiated silicon/electrolyte interface [36]. On the other hand, unlike the case of VC and FEC, VEC does not lead to safety improvement of graphite-based complete cells as observed by Ma et al. using ARC measurements [37]. Hence, each additive leads to characteristic thermal behavior changes which are due to the different chemical/thermal properties of the SEI layer compounds of polymeric or organic and inorganic nature. These interesting results reported in literature stress the relevance of undertaking an in-depth comparative study on the role of each additive on the negative electrode/electrolyte interface thermal behavior through the determination of the SEI texture/composition by analytical methods.

As aforementioned, in terms of thermal runaway, $LiPF_6$ plays a crucial role due to the formation of the PF_5 Lewis acid. In fact, Ryou et al. [38] have proved the influence of the salt by demonstrating the absence of reactivity between lithium alkyl carbonates and lithium bis(oxalate) borate (LiBOB) up to 150 °C in contrast to the exothermic reaction starting around 60 °C with $LiPF_6$. However, the limited solubility of LiBOB remains a critical drawback for considering this salt as a suitable alternative to $LiPF_6$ in commercial LiBs. Concerning the imide salts, our group has showed that acid-base reactions involving SEI components do not occur in the case of lithium bis(fluorosulfonyl)imide (LiFSI) salt but a sharp exothermic peak is observed with lithiated graphite powder at 200 °C due to FSI^- reduction [17].

Commercial negative electrodes consist of a film tape-cast on a copper foil, the film being composed of graphite (95–98%), conductive carbon (2–5%) and polymeric binders (2–5%). The role of binders on the thermal stability of graphite anodes has been studied by Park and al [7]. They showed that the heat energy release relative to the delithiation process is strongly diminished in the case of CMC/SBR or polyacrylic acid (PAA) binder, compared to PVDF binder. They assumed that this thermal stability improvement is due to the better coverage of the graphite particles, thanks to the strong interactions between functional groups of binder and graphite surface; the covering polymeric binder layer would have a lower lithium diffusivity than the SEI, slowing the thermally induced graphite delithiation. However, they only focused on the exothermic phenomena below 200 °C and did not take into account the reactivity of binders towards intercalated lithium as previously demonstrated in the case of PVDF [4].

Thanks to the numerous studies that have been devoted to the influence of binder, additive and salt components, it is clear that each of them plays a role on the thermal behavior of LiBs. However, identifying the contribution of each and comparing results with one another in a consistent way is quite difficult owing to differences in test samples (electrolyte and electrode composition …), techniques (DSC, C80, ARC …) and experimental protocols (sample preparation, heating ramp …) used in these studies.

To address these issues, we have carried out a comparative study where the same electrolyte (1 M $LiPF_6$ in EC:EMC:DMC (1:1:1 v/v/v)), and same negative electrode composite (graphite/Super P Carbon black/CMC/SBR 94/2/2/2 wt%) were used. Additionally, an optimized reliable experimental protocol was defined, allowing a high reproducibility of the DSC measurements. Using this configuration, our aim was to separate and trace back the origin of the contribution to exothermic reactions of CMC/SBR binder as well as the VEC, VC and FEC electrolyte additives, thanks to SEI characterization by means of FTIR and TEM. To complete this comparative study on critical components of LiBs under thermal abuse, the salt contribution was also studied through partial substitution of $LiPF_6$ by LiFSI, taking into account the aluminum corrosion issue [39].

2. Experimental

2.1. Materials

The reference electrolyte, purchased from Solvionic (France), is composed of 1 M $LiPF_6$ salt dissolved in a mixture of EC:DMC:EMC (1:1:1 v/v/v). Carbonate-based electrolyte test samples with salt mixtures of $LiPF_6$ (Aldrich, battery grade ≥ 99.99%) and LiFSI (Suzhou Fluolyte Co., purity > 99.9%) were prepared by adding the two salts in different molar ratios in EC:DMC:EMC (1:1:1 v/v/v, Solvionic) solvents mixture. Vinylene carbonate (VC), vinyl ethylene carbonate (VEC) and fluoroethylene carbonate (FEC) additives purchased from Sigma Aldrich (99% of purity) were added as 2 wt% level each to achieve final electrolytes composition for testing. The graphite powder electrode was composed of 90 wt% of natural graphite powder (d_{50}=19.4 μm, S.S.A. of 3 m^2/g, Hitachi) and 10 wt% of Super P carbon black (Timcal). The graphite film

electrode was composed of the same graphite powder with carboxymethyl cellulose (CMC, DS=0.67), styrene butadiene rubber (SBR) and Super P carbon black (94/2/2/2 wt%).

2.2. Cyclic voltammetry (CV)

The electrochemical stability of the electrolytes was measured by cyclic voltammetry in a three-electrode glass cell under argon atmosphere with a VMP-3 potentiostat-galvanostat (Biologic SA, Claix, France). The CV measurements were carried out from OCV to 6 V and reverse scan to 1.5 V vs. $Li^+/Li°$ at a scan rate of 30 mV/s using aluminum foil as working electrode and lithium and platinum wires as reference and counter electrodes, respectively.

2.3. Chronoamperometry (CA) and scanning electron microscopy (SEM)

Swagelok®-type cells were assembled in an argon-filled glove box using aluminum (1.27 cm^2) and lithium foils separated by 1 layer of Whatman GF/D borosilicate glass microfiber impregnated with 100 μL of electrolyte. Single potential measurements were performed at constant polarization potential of 4.15, 4.2 and 4.3 V vs. $Li^+/Li°$ during 15 h. Multi-potential chronoamperometry analysis was started at 4.15 V during 15 h followed by 7 h at 4.2 V and 7 h at 4.3 V vs. $Li^+/Li°$. After the experiments, the Swagelok cells were disassembled and Al current collectors were washed with acetonitrile into an ultrasonic cleaner prior to being analyzed using a scanning electron microscope Quanta 200FEG.

2.4. Cell assembling and cycling

Swagelok half cells were assembled in an argon-filled glove box. The graphite electrode was separated from the lithium metal foil by 1 layer of Whatman GF/D borosilicate glass microfiber impregnated with 50 μL of electrolyte, in the case of film electrode, and 2 layers of separator with 160 μL of electrolyte, when powder electrode is used. The galvanostatic discharge (graphite lithiation) was carried out at C/20 at 25 °C from OCV to 0.005 V vs. $Li^+/Li°$, followed by a charge to 1.5 V vs. $Li^+/Li°$ for FTIR and TEM analyzes, using the VMP-3 potentiostat-galvanostat.

2.5. Fourier transform infra-red (FTIR) spectroscopy

The charged cells were dismantled in an argon-filled glove box. Li_0C_6 powder was rinsed twice and dried under vacuum in the antechamber. Pellets were made by mixing a very small amount of Li_0C_6 powder with dry potassium bromide (KBr). The pellet mounted on the holder was also prepared in the glove box and put in a plastic bag. This was opened in the N_2-purged sample chamber of the FTIR system Nicolet 6700.

2.6. Transmission electron microscopy (TEM) analysis

The microstructural and structural study was performed using a transmission electron microscope FEI TECNAI F20 S-TWIN and Selected Area Electron Diffraction (SAED). In an argon-filled glove box, the rinsed and dried Li_0C_6 samples prepared for FTIR measurements were dispersed in DMC and deposited onto TEM copper grids with holey carbon. The samples were then transferred from the glove box to the TEM without air exposure.

2.7. Differential scanning calorimetry (DSC) measurements

After one lithiation, the Swagelok cells were disassembled in an argon-filled glove box. The lithiated graphite electrode impregnated with electrolyte was introduced and sealed in an aluminum crucible. Crucibles were pierced just prior to starting experiment. DSC measurements were performed in a Netzsch DSC 204F1 heat flux differential calorimeter at a heating rate of 10 °C/min under argon flow (200 mL/min). In order to ensure reproducibility, two DSC measurements were conducted on each sample.

3. Results and discussions

3.1. Thermal behavior of lithiated binder-free graphite/electrolyte

Before entering into a detailed investigation of the effect of binders, DSC experiments were first performed on lithiated graphite powder/electrolyte to provide a binder-free reference profile (Fig. 1). Note that, as for all DSC measurements of lithiated graphite, the two profiles presented on Fig. 1 evidence that the experiments are performed with high repeatability.

The heat energy release occurs within a temperature window from around 100 °C–325 °C. The first exothermic phenomenon between around 100 and 250 °C is well-known to involve the SEI breakdown followed by solvents reduction. The SEI breakdown, responsible for a very low energy release (as discussed later), was demonstrated to be mainly due to acid-base reactions (rxns 1–3) between SEI components and PF_5 [17], a $LiPF_6$ thermal decomposition product.

$$Li_2CO_3 + PF_5 \rightarrow 2\ LiF + POF_3 + CO_2 \quad (1)$$

$$(CH_2OCO_2Li)_2 + PF_5 \rightarrow 2\ LiF + C_2H_4F_2 + 2\ POF_3 + 2\ CO_2 \quad (2)$$

$$ROCO_2Li + PF_5 \rightarrow LiF + RF + POF_3 + CO_2\ (R{=}CH_3 \text{ or } C_2H_5) \quad (3)$$

The heat energy release still occurs beyond this temperature range. With the aim of discriminating the electrochemical and/or chemical origin of the relating thermal processes, DSC measurements of delithiated graphite were performed in the same conditions (Fig. 2a). As no intercalated lithium is available for solvent reduction, only a very small exothermic peak pertaining to the SEI decomposition is observed at 100 °C, followed by an endothermic peak due to EC evaporation. The absence of thermal phenomenon in the 250–300 °C range would let us assume that the heat energy release after 250 °C ensues exclusively from redox reactions occurring in this temperature range.

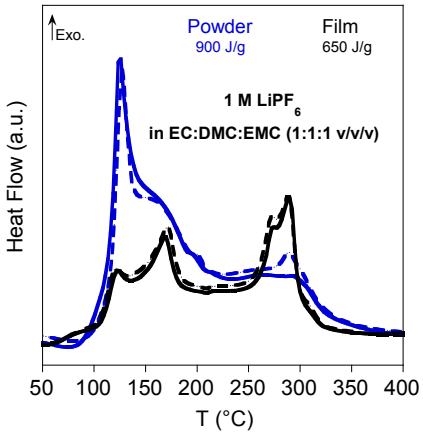

Fig. 1. DSC profiles of graphite/electrolyte after one lithiation in 1 M $LiPF_6$ EC:DMC:EMC (1:1:1 v/v/v) electrolyte without (blue) and with CMC/SBR binder (black), in open pan. (Reproducibility shown in dashed line). (For interpretation of the references to colour in this figure legend, the reader is referred to the web version of this article.)

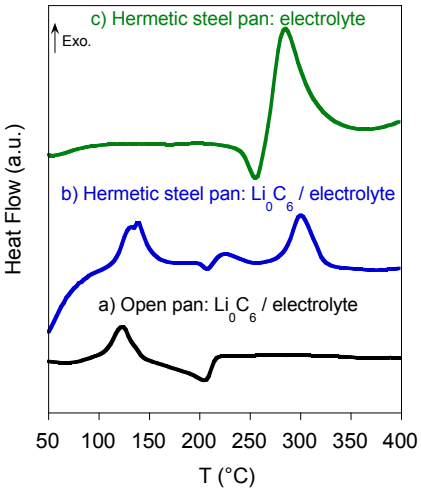

Fig. 2. DSC profiles of graphite/electrolyte after one lithiation/delithiation in 1 M $LiPF_6$ EC:DMC:EMC (1:1:1 v/v/v) electrolyte in a) open pan b) hermetic steel pan, and c) DSC profile of pure electrolyte in hermetic steel pan.

However, DSC profiles of electrolyte performed in hermetic steel pans, with and without delithiated graphite (Fig. 2 b and c), display an exothermic peak in the same 250–300 °C range, which is explained by PF_5 assisted polymerization of gaseous EC with CO_2 departure [33]. Hence, the high temperature exothermic phenomenon unveiled in case of lithiated graphite/electrolyte DSC measurements performed in open pan may be explained through both electrochemical and chemical processes: the presence of EC at such temperatures is made possible thanks to a particular confinement issuing from electrochemical reactions; the SEI breakdown is followed by solvents reduction bringing about the formation of a protective layer on the whole graphite surface, named secondary SEI. Therefore, according to the results obtained in hermetic steel pans, we assume that a small amount of gaseous EC, trapped in this secondary SEI or in the pores of the graphite, is maintained in this confined environment, and polymerizes in presence of PF_5 in the 250–300 °C range. Thus, electrolyte confinement to high temperature may result from the secondary SEI formation and the type of pan alike. Besides, regardless of the pan design, the heat generated after 250 °C is seemingly of chemical origin but requires electrochemical processes, occurring in the early temperature range.

3.2. Thermal behavior of CMC/SBR-based graphite film/electrolyte

In general, the use of a binder decreases the surface of graphite accessible to the electrolyte and consequently the irreversible capacity, associated to the SEI formation, compared to binder-free powder electrode. This graphite covering depends on the type of binder and more precisely on its affinity with graphite surface functional groups. On the safety point of view, depending on the type of binder, additional exothermic phenomena may take place due to possible thermal instability of the binder itself or its reactivity towards other components at elevated temperature.

In the case of a graphite electrode containing polyvinylidene difluoride (PVDF), alone thermally stable up to 400 °C, Du Pasquier et al. [4] assumed that the exothermic process observed in DSC at temperatures higher than 280 °C is due to the following redox reaction between LiC_6 and the PVDF binder:

$$-CH_2-CF_2- + Li \rightarrow LiF + -CH{=}CF- + \tfrac{1}{2}\, H_2$$

The reactivity of PVDF towards Li was supported by other groups [14,15,18] and compared to other binders as phenol-formaldehyde (PF), ethylenepropylene-diene (EPD) and copolymer of vinylidene fluoride (VDF). However, in more recent studies [19,20] this sharp exothermic peak around 280 °C was attributed to the reaction between LiC_6 and electrolyte on the basis of the absence of this peak after a washing-drying procedure.

In our case, composite electrode films are made of graphite, carbon Super P, CMC and SBR. As suggested in the case of polyacrylic acid (PAA) binder by K. Ui et al. [40], the carboxyl groups of CMC binder react with functional groups at the edge of the graphite to give ester bonds, reducing the surface accessible to the electrolyte. Therefore, it is generally expected that the use of CMC/SBR binder leads to a smaller irreversible capacity during the first cycle and also to a smaller heat release relating to the SEI decomposition in the early stage of the exothermic phenomena (100–250 °C range) [7].

DSC profile of the lithiated CMC/SBR-based graphite film in presence of electrolyte is presented in Fig. 1. Both powder and film electrodes exothermic phenomena are found to extend over the same broad temperature range (100–325 °C) however displaying a strong influence of the binder on the profile intensity, as well as on the overall heat generation. The total heat energy release for lithiated graphite film is calculated to be 650 J/g (the copper mass being removed), which corresponds to a decrease of 250 J/g compared to the powder electrode. As expected from previous assumptions regarding the covering role of the binder, the first exothermic phenomenon has significantly shrunk. However, this beneficial effect of CMC/SBR binder on the thermal behavior of lithiated graphite/electrolyte below 200 °C is accompanied by a small increase of the exothermic phenomena in the 250–300 °C range.

This latter peak which was previously attributed to EC polymerization in the case of binder-free graphite powder seems to overlap with another peak in the presence of CMC/SBR binder. In order to suppress the electrolyte induced heat generation in this temperature range, the electrolyte impregnating the lithiated graphite film electrode pores was removed by a rinsing with acetonitrile and drying procedure prior to thermal measurements. The DSC profile of the lithiated graphite film electrode without electrolyte, displayed in Fig. 3a, shows an exothermic peak at 290 °C which is not present in the case of fresh graphite film electrode (Fig. 3d). This result seems to indicate that the composite film electrode reacts with the remaining intercalated lithium at this temperature.

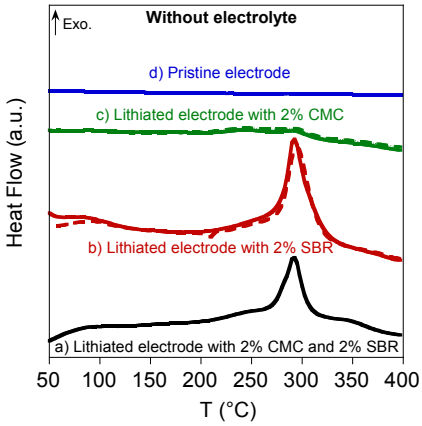

Fig. 3. DSC profiles of graphite electrode after one lithiation in 1 M $LiPF_6$ EC:DMC:EMC (1:1:1 v/v/v) electrolyte after a washing-drying procedure a) with CMC/SBR, b) with only SBR, c) with only CMC and d) pristine electrode, in open pan.

As an attempt to identify which of the binder polymers (CMC or SBR) is thermally active in this temperature range, films with same graphite (96 wt%) and Super P carbon black (2 wt%) were prepared with either CMC or SBR (2 wt%) alone. DSC profile of the CMC film without SBR in absence of electrolyte (Fig. 3c) reveals no exothermic peak in the 250–300 °C range, which demonstrates the absence of reaction between intercalated lithium and CMC. In contrast, when SBR is used alone (Fig. 3b), an exothermic peak is observed in this temperature range, as for the reference film (Fig. 3a), suggesting a possible reaction between intercalated lithium and SBR. However, as a SBR reduction reaction seems hardly conceivable, a deeper investigation is under progress to know its specific role in this thermal phenomenon.

The overall DSC measurements have demonstrated that, despite the exothermic redox reaction involving SBR and lithium above 250 °C, the presence of the CMC coating of graphite particles has a positive effect on the thermal stability of LiC_6 film/electrolyte in the 100–250 °C range. In the next part, the question arises as to whether or not the electrolyte additive such as VC, VEC and FEC could still improve the thermal stability of lithiated graphite in presence of electrolyte.

3.3. Influence of electrolyte additives: VC, VEC and FEC

The carbonate additives VC, VEC and FEC are classified as SEI forming improver additives [41]. They exhibit a lower LUMO energy level compared to solvents and therefore are reduced at higher potential. Hence, as their insoluble reduction products are part of the SEI, their use could further retard the SEI breakdown induced electrolyte reduction.

From the first graphite powder lithiation/delithiation potential profile (Fig. 4), it has to be noticed that the amount of intercalated lithium is the same regardless of electrolyte. The additives reduction potentials can be sorted in the following order: E_{red} vs. Li^+/Li: VEC > FEC > VC > solvents (principally EC at 0.8 V vs. Li^+/Li). Moreover, according to the derivative plots vs. potential (Fig. 4 inset), the solvents reduction seems not to be totally hindered. In fact, the reduction peak of VC overlaps with the one observed in the case of the reference electrolyte. The reduction of VEC and FEC which takes place around 1.4–1 V and 1.3–0.9 V respectively, is followed by a small peak in the solvents reduction potential range (0.9–0.7 V vs. Li^+/Li). Nevertheless, the decrease of the solvent reduction peak reflects some modifications of the classical SEI emanating from the presence of non-soluble additives reduction products that we attempted to analyze by making use of FTIR and TEM techniques.

All Li_0C_6 FTIR spectra (Fig. 4) unveil expected bands assigned in the literature [42–45] to lithium carbonate and lithium ethyl dicarbonate at 1500, 1445 and 870 cm^{-1} and 1650, 1300, 1090 and 825 cm^{-1} respectively. Despite the fact that FTIR analysis is not a quantitative method, the relative intensity of lithium carbonate bands when VEC is used indicates that Li_2CO_3 is the major reduction product of VEC [46]. According to the TEM images of Li_0C_6, the entire graphite surface is covered by a highly irregular layer with a thickness ranging from 20 to 90 nm (Fig. 5b). This Li_2CO_3 layer is much less homogeneous than the solvents reduction-induced SEI (average of 10–25 nm) (Fig. 5a). When VC is added to the electrolyte, additional FTIR bands are observed at 1800, 1580 and 1300 cm^{-1} resulting from the formation of poly(vinylene carbonate) [47,48] via an anionic polymerization process. The TEM image (Fig. 5c) shows a smooth and uniform 10 nm thick SEI layer which covers perfectly the whole surface of graphite. In the case of FEC, no drastic change is observed compared to the reference infrared spectrum, except the increase in intensity of the 1580 cm^{-1} band suggesting the presence of polyacetylene (υC=C).

According to the FEC reduction mechanism described below, polyacetylene should form along with LiF and Li_2CO_3 compounds [49]. This mechanism is supported by the TEM image (Fig. 5d) which presents a SEI layer composed of both a uniform 3–5 nm thick film and numerous porous polycrystalline spherical particles of approximately 100 nm diameter. The SAED pattern (not shown here) of these spherical particles was successfully indexed as LiF. The deduced reduction mechanisms of VEC, VC and FEC illustrated in Scheme 1 highlight quite different SEI compositions which may impact the LiC_6/electrolyte thermal behavior.

DSC measurements performed on lithiated graphite film electrode/electrolyte samples clearly show that the addition of any additive, VC, VEC or FEC (Fig. 6), allows to decrease the heat energy release by at least 150 J/g compared to the reference (Table 1). The addition of VEC does not influence the onset temperature as

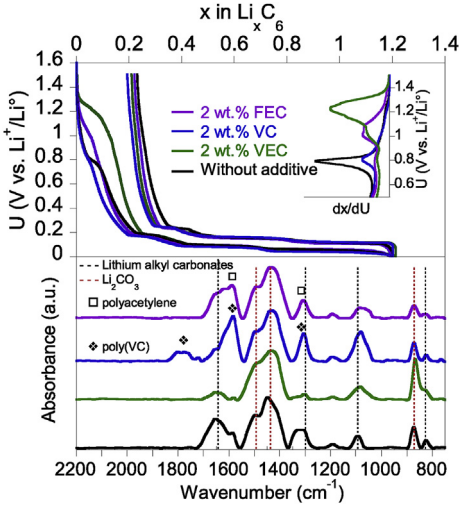

Fig. 4. Galvanostatic traces (top) of the first lithiation/delithiation of graphite powder in 1 M $LiPF_6$ EC:DMC:EMC (1:1:1 v/v/v) electrolyte without and with 2 wt% of VEC, VC or FEC (derivative plots in inset). FTIR spectra (bottom) of these delithiated graphite powders after a washing-drying procedure.

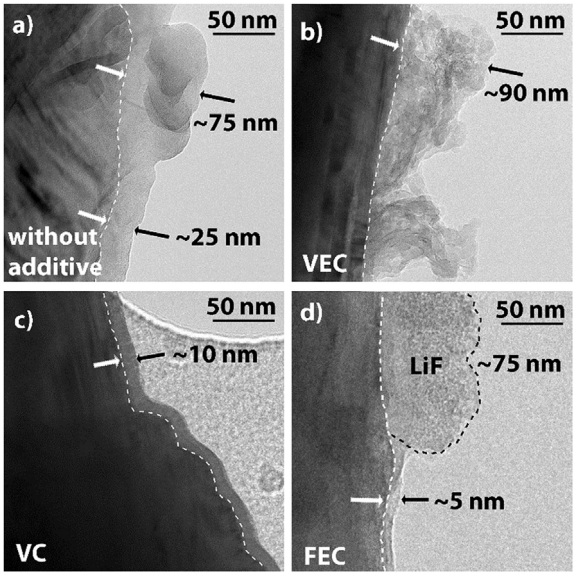

Fig. 5. TEM images of graphite after one lithiation/delithiation in 1 M $LiPF_6$ EC:DMC:EMC (1:1:1 v/v/v) electrolyte a) without and with 2 wt% of b) VEC, c) VC and d) FEC.

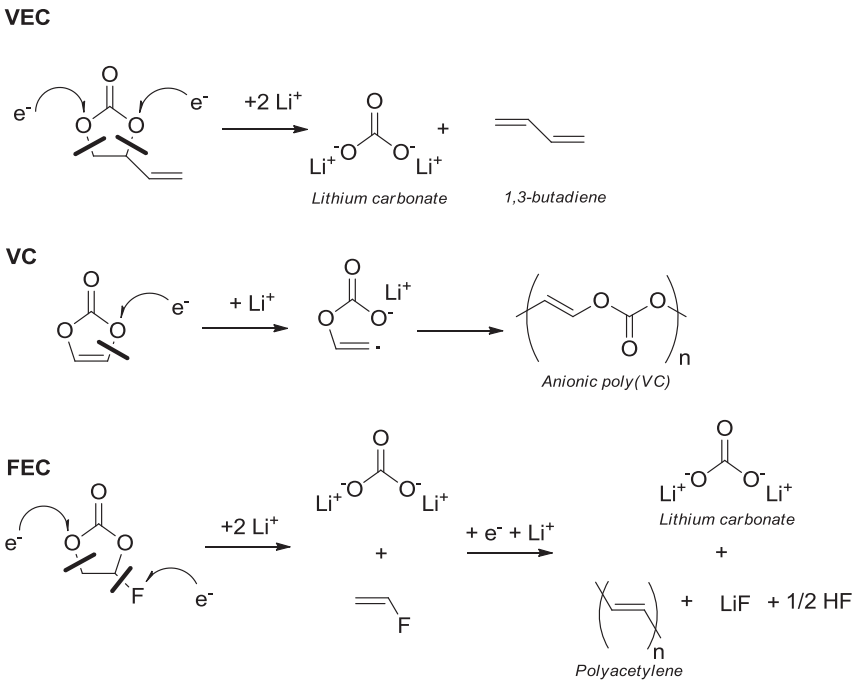

Scheme 1. Reduction mechanisms of VEC, VC and FEC additives.

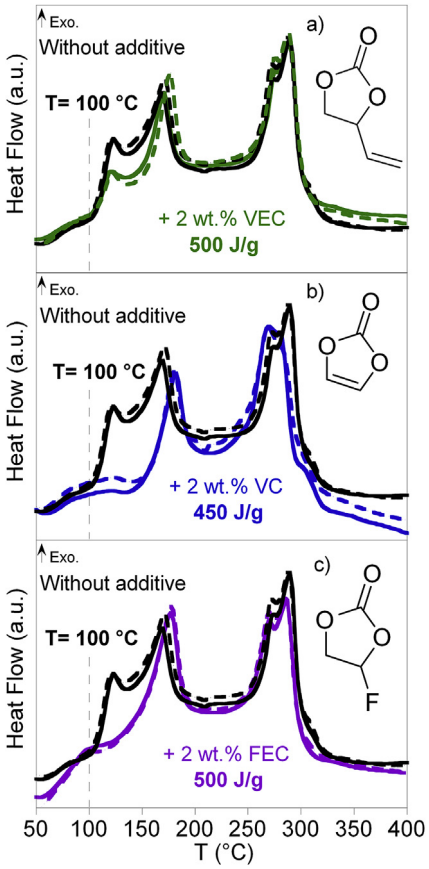

Fig. 6. DSC profiles of graphite/electrolyte after one lithiation in 1 M $LiPF_6$ EC:DMC:EMC (1:1:1 v/v/v) electrolyte with 2 wt% of a) VEC, b) VC and c) FEC compared to that without additive (black), in open pan. (Reproducibility shown in dashed line).

expected from the FTIR analysis of the SEI composition. In fact, in presence of VEC, as Li_2CO_3 is the major part of the SEI, the feasibility of the reaction between Li_2CO_3 and PF_5, responsible of the onset temperature at 100 °C, is therefore not affected. However, the thickness of this layer delays the electrolyte accessibility to lithiated graphite, favoring the departure of linear carbonates outside the DSC pan at the expense of their reduction, which consequently explains a lower heat energy release in the 100–150 °C range. When VC or FEC is added, the onset temperature of the first exothermic phenomenon is shifted to a higher value by +50 °C and +20 °C, respectively. In the case of VC, the whole graphite surface is covered by a uniform polymeric layer which delays the access of the electrolyte to the intercalated lithium into graphite and decreases the total heat energy release. FEC reduction results in many LiF spherical particles with polyacetylene film leading to a non-homogeneous graphite coverage which is somewhat less effective to prevent the electrolyte reduction upon heating. It has to be noticed that even if some Li_2CO_3 is detected by FTIR, its amount is not significant enough or not accessible to generate an exothermic peak at 100 °C on the DSC profile (Fig. 6b and c).

In brief, despite the exothermic redox reaction involving SBR and lithium above 250 °C, CMC/SBR binder and VEC, VC or FEC electrolyte additives were found to improve the thermal behavior of LiC_6/electrolyte through a partial effective coverage of the graphite surface and a modification of the SEI chemical composition/thickness respectively. Among the tested additives, VC proved to be the most efficient additive from a safety point of view with the lowest heat release and highest onset temperature. As the protocol used has allowed to accurately define the thermal impact of a chemical change, we have further pursued our investigation, considering the partial substitution of $LiPF_6$ salt by LiFSI as a possibility to reduce the PF_5 formation responsible for the SEI breakdown.

3.4. Influence of the salt substitution by LiFSI

Among the alternatives investigated so far, namely borate salts

Table 1
Summary of SEI characterization and LiC_6/electrolyte thermal behavior as a function of electrolyte: 1 M $LiPF_6$ EC:DMC:EMC (1:1:1 v/v/v) without additive and with 2 wt% of VEC, VC or FEC.

Electrolyte 1 M $LiPF_6$ in EC:DMC:EMC (1:1:1 v/v/v)		Without additive	+2 wt% VEC	+2 wt% VC	+2 wt% FEC
SEI characterization	Composition deduced from IR and/or TEM	Li_2CO_3 + lithium alkyl carbonates	Li_2CO_3 + traces of lithium alkyl carbonates	-$(OCO_2CH{=}CH)_n$- + Li_2CO_3 and lithium alkyl carbonates	LiF + -$(CH{=}CH)_n$- + Li_2CO_3 and lithium alkyl carbonates
	Thickness	10–25 nm	≈20–90 nm	10 nm	Film: 3–5 nm, LiF: ≈ 100 nm
Thermal behavior	T_{onset}	100 °C	100 °C	150 °C	120 °C
	$E_{released}$ (±50 J/g)	650	500	450	500

(lithium tetrafluoroborate ($LiBF_4$) [50,51], lithium bis(oxalato) borate (LiBOB) [50,52,53], lithium difluoro(oxalate)borate (LiDFOB) [50,54] …) and imide salts (lithium bis(trifluoromethanesulfonyl) imide (LiTFSI) [50,55], lithium bis(fluorosulfonyl)imide (LiFSI) [39,50,56,57] …), the LiFSI ($Li(SO_2F)_2N$) salt is reported to be the best candidate to replace $LiPF_6$ thanks to its higher ionic conductivity, better stability towards hydrolysis and lower fluorine content compared to $LiPF_6$. However, the main drawback of this imide salt is its inability to protect the aluminum current collector from corrosion beyond 4 V [39].

In fact, the native air-formed oxide (Al_2O_3, $Al(OH)_3$) film observed on an aluminum current collector (2–5 nm thickness) acts as a protection layer against aluminum oxidation up to 4 V using conventional Li-ion battery electrolytes. At higher potential, owing to the presence of $LiPF_6$ salt, a more passivating AlF_3 layer is formed on the top of this oxide layer by the reaction of Al_2O_3 with HF and/or Al^{3+} ions with F^-, blocking subsequent aluminum oxidation [58]. The thin surface film of AlF_3 (~2 nm) provides significant resistance to corrosion. In contrast, with LiFSI salt containing electrolyte, the film formed on the surface of aluminum is non-protective and aluminum corrosion takes place, probably due to the solubility of $[(FSO_2)_2N]_3Al$ [39]. As a possible solution to overcome this problem is the use of LiFSI/$LiPF_6$ salts mixture [59], we embarked into a preliminary corrosion study to determine the best ratio to use before appraising the presumed further improvement of the lithiated graphite CMC/SBR film/electrolyte thermal stability while decreasing the $LiPF_6$ content.

So, the electrochemical potential window of electrolytes with LiFSI (1 M) and different molar concentrations of $LiPF_6$ + LiFSI (0.5 + 0.5; 0.6 + 0.4; 0.66 + 0.33) were first assessed by means of CV measurements. Voltammograms (Fig. 7a) reveal aluminum corrosion from 3.3, 3.8 and 4 V vs. Li^+/Li with LiFSI (1 M) and 0.5 + 0.5 and 0.6 + 0.4 M concentrations of $LiPF_6$ + LiFSI respectively. In contrast, no characteristic anodic current is observed in the case of the 0.66 + 0.33 M concentration, reflecting the absence of corrosion in these conditions.

In order to support this outcome, chronoamperometry analyzes were performed on the electrolyte containing the optimized composition (0.66 + 0.33 M concentration of $LiPF_6$ + LiFSI) at 4.15, 4.2 and 4.3 V during 15 h (Fig. 7b). After polarization at 4.15 and 4.2 V vs. Li^+/Li, the residual current drops below 1 μA/cm^2 after ca. 1 h, and continues to decrease until the end of the experiment, demonstrating no aluminum oxidation process (confirmed by SEM analyzes not shown here). In contrast, the polarization directly to 4.3 V leads to a current higher than 5 μA/cm^2 during the whole experiment, resulting from aluminum oxidation (Fig. 7b inset). The aluminum protection up to 4.2 V, thanks to the AlF_3 layer formed in the presence of $LiPF_6$, renders possible the use of this electrolyte with cells containing layered $LiCoO_2$ (LCO) and $LiNi_yMn_yCo_{1-2y}O_2$ (NMC) cathodes. Nevertheless, it must be stressed that applying a preliminary multi-potential chronoamperometry step has turned out to be efficient in increasing the corrosion potential beyond 4.2 V. Indeed, the current remains very low (≈0.1 μA/cm^2) at 4.3 V after a multi-step polarization at 4.15 and 4.2 V potentials during 15 h and 7 h, respectively (Fig. 7c). The formation of a protective AlF_3 layer seems to be achieved during the first polarization steps and no further Al corrosion is observed by SEM on the aluminum current collector after polarization up to 4.3 V (Fig. 7c inset). Hence, the use of 0.66 + 0.33 M concentration of $LiPF_6$ + LiFSI in spinel $LiMn_2O_4$ cathode containing cells may be envisaged with an appropriate polarization procedure. From these results, it has to be noticed that the CV measurement is not sufficient to demonstrate the non-corrosive behavior of the $LiPF_6$ and LiFSI salts mixture whereas, using appropriate experimental conditions, the CA analysis can be more accurate.

This preliminary study demonstrated that $LiPF_6$-based electrolytes can be only partially substituted by LiFSI salt up to a maximum of 33% in case of 1 M lithium salt concentration. Therefore, this ratio has been chosen for comparative DSC investigations.

According to Eshetu et al. [17], DSC measurements carried out on LiC_6 powder/LiFSI (1 M) containing electrolyte unveil a sharp and highly exothermic phenomenon around 200 °C due to the electrochemical reduction of LiFSI. Hence, as the CMC/SBR binders were found to positively impact the thermal behavior with $LiPF_6$-based electrolyte, the same experiments were performed on both powder and film electrodes with pure LiFSI electrolyte (Fig. 8d and e) as a preliminary step to the study of the role of the salts blend.

As expected, the sharp exothermic peak, observed in the case of powder electrode, is very less pronounced in presence of the binders, which, once again, highlights their role in limiting contact between LiC_6 and electrolyte.

The thermal stability of this lithiated graphite film was then tested in the presence of the 0.66 M $LiPF_6$ + 0.33 M LiFSI electrolyte,

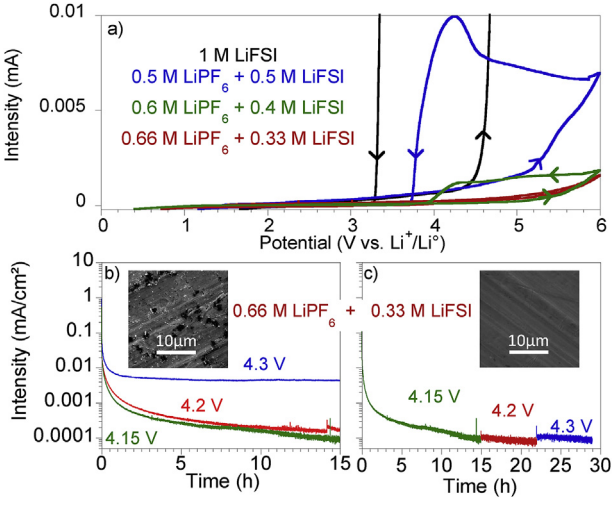

Fig. 7. a) Cyclic voltammograms of electrolyte containing 1 M LiFSI, 0.5 M $LiPF_6$ + 0.5 M LiFSI, 0.6 M $LiPF_6$ + 0.4 M LiFSI and 0.66 M $LiPF_6$ + 0.33 M LiFSI. Chronoamperograms of aluminum film polarized at b) 4.15, 4.2 and 4.3 V vs. Li^+/Li° during 15 h and c) at 4.15, 4.2 and 4.3 V vs. Li^+/Li° during 15, 7 and 7 h respectively, in EC:DMC:EMC (1:1:1 v/v/v) with 0.66 M $LiPF_6$ + 0.33 M LiFSI. MEB images of aluminum film after polarization at 4.3 V in inset.

with 2 wt% of VC, this one being identified as the best additive in the previous part (Fig. 8c). The beneficial effect of VC (Fig. 8b), i.e. a + 50 °C shift of the onset temperature compared to the reference (Fig. 8a), is preserved when 33% of $LiPF_6$ salt is replaced by LiFSI. Moreover, the partial substitution of $LiPF_6$ by LiFSI leads to a decrease of the exothermic peak starting at 150 °C, which can be explained by the smaller amount of PF_5, coming from $LiPF_6$ thermal degradation or to the different SEI composition due to FSI^- reduction. The thermal behavior of LiC_6/electrolyte is improved by the synergistic effect of VC addition and the partial substitution of $LiPF_6$ by LiFSI.

4. Conclusion

The role that the state-of-the-art electrode binders, carbonate additives and lithium salt do play on the thermal runaway of LiBs has been accurately assessed using DSC, TEM and FTIR techniques and discriminating testing protocols.

This study allowed to determine to what extent the SBR/CMC binder polymers modify the thermal reactivity of a lithiated graphite powder in contact with electrolyte. Indeed, a lower heat energy released with a more steady flow over the same temperature range (100–325 °C) has been observed, which may favor better energy dissipation upon a thermal runaway. Besides, a chemical reaction between intercalated lithium and SBR above 250 °C was revealed and further investigations are ongoing to get better insight into reaction mechanisms.

The studied carbonate-type SEI-improver additives were found to all have a beneficial effect on the SBR/CMC-based negative electrode thermal behavior through an increase of SEI thickness (VEC) or the formation of polymers (VC and FEC). However, the polymeric nature of the VC-derived SEI and its homogeneous texture were found to provide the most efficient graphite coverage from the point of view of safety.

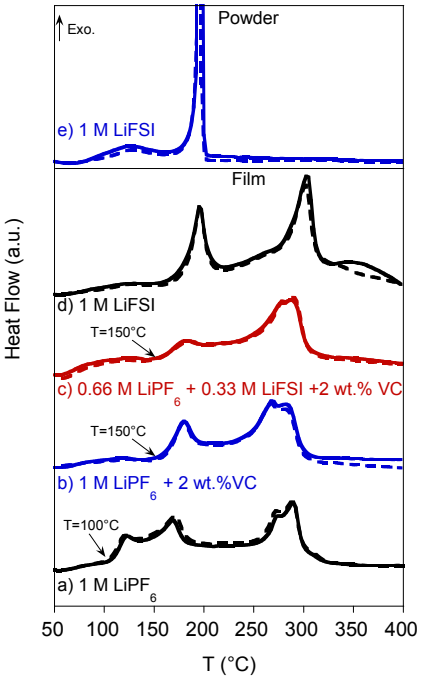

Fig. 8. DSC profiles of graphite film/electrolyte after one lithiation in EC:DMC:EMC (1:1:1 v/v/v) solvent with a) 1 M $LiPF_6$, b) 1 M $LiPF_6$ with 2 wt% of VC, c) 0.66 M $LiPF_6$ + 0.33 M LiFSI with 2 wt% of VC, d) 1 M LiFSI and e) 1 M LiFSI in the case of graphite powder/electrolyte, in open pan. (Reproducibility shown in dashed line).

Finally, we demonstrated that LiFSI, with an optimal salt ratio of 0.66 M $LiPF_6$ and 0.33 M LiFSI, can be used without facing any aluminum corrosion issue up to 4.3 V vs. $Li^+/Li°$, enabling its use with NMC111 as positive electrode in Li-ion batteries. Moreover, with 2 wt% of VC added in this electrolyte composition, it has been shown that the thermal behavior of graphite electrode was slightly improved compared to an identical solvents mixture with 1 M $LiPF_6$. This result turned out to be quite promising while considering the known highly exothermic peak revealed in case of graphite powder/LiFSI 1 M electrolyte thermal reactivity.

All highlighted improvements in terms of intrinsic safety margins against thermal runaway potentially achievable by appropriate component selection from such DSC analysis are currently being verified on complete cells, taking into account the additional contribution from other battery components (cathode and separator). Subsequent results will be the subject of a forthcoming paper.

In addition, this methodology providing valuable data on SEIs and thermal behaviors should be helpful for next generation negative materials (LTO, Si-C, hard carbon for Na-ion battery …) investigations.

Acknowledgments

Support from the Association Nationale de la Recherche et de la Technologie is gratefully acknowledged. We also thank Carine Lenfant for proofreading this paper.

References

[1] FS_Safety Issues for Lithium-Ion Batteries_10-12.pdf, (n.d.). http://www.ul.com/global/documents/newscience/whitepapers/firesafety/FS_Safety%20Issues%20for%20Lithium-Ion%20Batteries_10-12.pdf.
[2] G. Gachot, S. Grugeon, I. Jimenez-Gordon, G.G. Eshetu, S. Boyanov, A. Lecocq, G. Marlair, S. Pilard, S. Laruelle, Gas chromatography/Fourier transform infrared/mass spectrometry coupling: a tool for Li-ion battery safety field investigation, Anal. Methods 6 (2014) 6120, http://dx.doi.org/10.1039/C4AY00054D.
[3] H. Maleki, G. Deng, A. Anani, J. Howard, Thermal stability studies of Li-Ion cells and components, J. Electrochem. Soc. 146 (1999) 3224–3229.
[4] A.D. Pasquier, F. Disma, T. Bowmer, A.S. Gozdz, G. Amatucci, J.-M. Tarascon, Differential scanning calorimetry study of the reactivity of carbon anodes in plastic Li-Ion batteries, J. Electrochem. Soc. 145 (1998) 472–477, http://dx.doi.org/10.1149/1.1838287.
[5] A.M. Andersson, M. Herstedt, A.G. Bishop, K. Edström, The influence of lithium salt on the interfacial reactions controlling the thermal stability of graphite anodes, Electrochim. Acta 47 (2002) 1885–1898.
[6] G. Gachot, S. Grugeon, G.G. Eshetu, D. Mathiron, P. Ribière, M. Armand, S. Laruelle, Thermal behaviour of the lithiated-graphite/electrolyte interface through GC/MS analysis, Electrochim. Acta 83 (2012) 402–409, http://dx.doi.org/10.1016/j.electacta.2012.08.016.
[7] Y.-S. Park, E.-S. Oh, S.-M. Lee, Effect of polymeric binder type on the thermal stability and tolerance to roll-pressing of spherical natural graphite anodes for Li-ion batteries, J. Power Sources 248 (2014) 1191–1196, http://dx.doi.org/10.1016/j.jpowsour.2013.10.076.
[8] G.G. Botte, R.E. White, Z. Zhang, Thermal stability of LiPF6–EC: EMC electrolyte for lithium ion batteries, J. Power Sources 97–98 (2001) 570–575, http://dx.doi.org/10.1016/S0378-7753(01)00746-7.
[9] T. Kawamura, A. Kimura, M. Egashira, S. Okada, J.-I. Yamaki, Thermal stability of alkyl carbonate mixed-solvent electrolytes for lithium ion cells, J. Power Sources 104 (2002) 260–264.
[10] B. Ravdel, K. Abraham, R. Gitzendanner, J. DiCarlo, B. Lucht, C. Campion, Thermal stability of lithium-ion battery electrolytes, J. Power Sources 119–121 (2003) 805–810, http://dx.doi.org/10.1016/S0378-7753(03)00257-X.
[11] Z. Lu, L. Yang, Y. Guo, Thermal behavior and decomposition kinetics of six electrolyte salts by thermal analysis, J. Power Sources 156 (2006) 555–559, http://dx.doi.org/10.1016/j.jpowsour.2005.05.085.
[12] J. Lamb, C.J. Orendorff, E.P. Roth, J. Langendorf, Studies on the thermal breakdown of common Li-Ion battery electrolyte components, J. Electrochem. Soc. 162 (2015) A2131–A2135.
[13] R. Spotnitz, J. Franklin, Abuse behavior of high-power, lithium-ion cells, J. Power Sources 113 (2003) 81–100.
[14] P. Biensan, B. Simon, J. Pérès, A. de Guibert, M. Broussely, J. Bodet, F. Perton, On safety of lithium-ion cells, J. Power Sources 81–82 (1999) 906–912, http://

dx.doi.org/10.1016/S0378-7753(99)00135-4.
[15] Z. Zhang, D. Fouchard, J.R. Rea, Differential scanning calorimetry material studies: implications for the safety of lithium-ion cells, J. Power Sources 70 (1998) 16–20.
[16] J. Yamaki, H. Takatsuji, T. Kawamura, M. Egashira, Thermal stability of graphite anode with electrolyte in lithium-ion cells, Solid State Ion. 148 (2002) 241–245.
[17] G.G. Eshetu, S. Grugeon, G. Gachot, D. Mathiron, M. Armand, S. Laruelle, LiFSI vs. LiPF6 electrolytes in contact with lithiated graphite: comparing thermal stabilities and identification of specific SEI-reinforcing additives, Electrochim. Acta 102 (2013) 133–141, http://dx.doi.org/10.1016/j.electacta.2013.03.171.
[18] H. Maleki, G. Deng, I. Kerzhner-Haller, A. Anani, J.N. Howard, Thermal stability studies of binder materials in anodes for lithium-ion batteries, J. Electrochem. Soc. 147 (2000) 4470–4475.
[19] E. Roth, D. Doughty, J. Franklin, DSC investigation of exothermic reactions occurring at elevated temperatures in lithium-ion anodes containing PVDF-based binders, J. Power Sources 134 (2004) 222–234, http://dx.doi.org/10.1016/j.jpowsour.2004.03.074.
[20] H. Yang, H. Bang, K. Amine, J. Prakash, Investigations of the exothermic reactions of natural graphite anode for Li-Ion batteries during thermal runaway, J. Electrochem. Soc. 152 (2005) A73, http://dx.doi.org/10.1149/1.1836126.
[21] H. Arai, M. Tsuda, K. Saito, M. Hayashi, Y. Sakurai, Thermal reactions between delithiated lithium nickelate and electrolyte solutions, J. Electrochem. Soc. 149 (2002) A401, http://dx.doi.org/10.1149/1.1452114.
[22] D.D. MacNeil, T.D. Hatchard, J.R. Dahn, A Comparison between the High Temperature Electrode/Electrolyte Reactions of Li[sub x]CoO[sub 2] and Li[sub x]Mn[sub 2]O[sub 4], J. Electrochem. Soc. 148 (2001) A663, http://dx.doi.org/10.1149/1.1375798.
[23] Y. Wang, J. Jiang, J.R. Dahn, The reactivity of delithiated Li(Ni1/3Co1/3Mn1/3)O2, Li(Ni0.8Co0.15Al0.05)O2 or LiCoO2 with non-aqueous electrolyte, Electrochem. Commun. 9 (2007) 2534–2540, http://dx.doi.org/10.1016/j.elecom.2007.07.033.
[24] Y. Baba, Thermal stability of LixCoO2 cathode for lithium ion battery, Solid State Ion. 148 (2002) 311–316, http://dx.doi.org/10.1016/S0167-2738(02)00067-X.
[25] Y.-C. Jung, S.-K. Kim, M.-S. Kim, J.-H. Lee, M.-S. Han, D.-H. Kim, W.-C. Shin, M. Ue, D.-W. Kim, Ceramic separators based on Li+-conducting inorganic electrolyte for high-performance lithium-ion batteries with enhanced safety, J. Power Sources 293 (2015) 675–683, http://dx.doi.org/10.1016/j.jpowsour.2015.06.001.
[26] C.J. Orendorff, The role of separators in lithium-ion cell safety, Electrochem. Soc. Interface 21 (2012) 61–65.
[27] V. Eshkenazi, E. Peled, L. Burstein, D. Golodnitsky, XPS analysis of the SEI formed on carbonaceous materials, Solid State Ion. 170 (2004) 83–91, http://dx.doi.org/10.1016/S0167-2738(03)00107-3.
[28] D. Aurbach, Y. Ein-Eli, B. Markovsky, A. Zaban, S. Luski, Y. Carmeli, H. Yamin, The study of electrolyte solutions based on ethylene and diethyl carbonates for rechargeable Li batteries ii. Graphite electrodes, J. Electrochem. Soc. 142 (1995) 2882–2890.
[29] E. Peled, The electrochemical behavior of alkali and alkaline earth metals in nonaqueous battery systems—the solid electrolyte interphase model, J. Electrochem. Soc. 126 (1979) 2047, http://dx.doi.org/10.1149/1.2128859.
[30] S.F. Lux, I.T. Lucas, E. Pollak, S. Passerini, M. Winter, R. Kostecki, The mechanism of HF formation in LiPF6 based organic carbonate electrolytes, Electrochem. Commun. 14 (2012) 47–50, http://dx.doi.org/10.1016/j.elecom.2011.10.026.
[31] H. Yang, G.V. Zhuang, P.N. Ross, Thermal stability of LiPF6 salt and Li-ion battery electrolytes containing LiPF6, J. Power Sources 161 (2006) 573–579, http://dx.doi.org/10.1016/j.jpowsour.2006.03.058.
[32] S.E. Sloop, J.K. Pugh, S. Wang, J.B. Kerr, K. Kinoshita, Chemical reactivity of PF[sub 5] and LiPF[sub 6] in ethylene carbonate/dimethyl carbonate solutions, Electrochem. Solid-State Lett. 4 (2001) A42, http://dx.doi.org/10.1149/1.1353158.
[33] S.E. Sloop, J.B. Kerr, K. Kinoshita, The role of Li-ion battery electrolyte reactivity in performance decline and self-discharge, J. Power Sources 119–121 (2003) 330–337, http://dx.doi.org/10.1016/S0378-7753(03)00149-6.
[34] K. Tasaki, K. Kanda, S. Nakamura, M. Ue, Decomposition of LiPF[sub 6] and stability of PF[sub 5] in Li-Ion battery electrolytes, J. Electrochem. Soc. 150 (2003) A1628, http://dx.doi.org/10.1149/1.1622406.
[35] S. Amiruddin, J. Prakash, H.J. Bang, K. Amine, The effect of vinylene carbonate (VC) on the thermal behavior of carbon fiber (CF) anode, ECS (2007) 41–47, http://dx.doi.org/10.1149/1.2409026.
[36] I.A. Profatilova, C. Stock, A. Schmitz, S. Passerini, M. Winter, Enhanced thermal stability of a lithiated nano-silicon electrode by fluoroethylene carbonate and vinylene carbonate, J. Power Sources 222 (2013) 140–149, http://dx.doi.org/10.1016/j.jpowsour.2012.08.066.
[37] L. Ma, J. Xia, X. Xia, J.R. Dahn, The impact of vinylene carbonate, fluoroethylene carbonate and vinyl ethylene carbonate electrolyte additives on electrode/electrolyte reactivity studied using accelerating rate calorimetry, J. Electrochem. Soc. 161 (2014) A1495–A1498.
[38] M.-H. Ryou, J.-N. Lee, D.J. Lee, W.-K. Kim, Y.K. Jeong, J.W. Choi, J.-K. Park, Y.M. Lee, Effects of lithium salts on thermal stabilities of lithium alkyl carbonates in SEI layer, Electrochim. Acta 83 (2012) 259–263, http://dx.doi.org/10.1016/j.electacta.2012.08.012.
[39] L. Li, S. Zhou, H. Han, H. Li, J. Nie, M. Armand, Z. Zhou, X. Huang, Transport and electrochemical properties and spectral features of non-aqueous electrolytes containing LiFSI in linear carbonate solvents, J. Electrochem. Soc. 158 (2011) A74, http://dx.doi.org/10.1149/1.3514705.
[40] K. Ui, D. Fujii, Y. Niwata, T. Karouji, Y. Shibata, Y. Kadoma, K. Shimada, N. Kumagai, Analysis of solid electrolyte interface formation reaction and surface deposit of natural graphite negative electrode employing polyacrylic acid as a binder, J. Power Sources 247 (2014) 981–990, http://dx.doi.org/10.1016/j.jpowsour.2013.08.083.
[41] S.S. Zhang, A review on electrolyte additives for lithium-ion batteries, J. Power Sources 162 (2006) 1379–1394, http://dx.doi.org/10.1016/j.jpowsour.2006.07.074.
[42] S.A. Freunberger, Y. Chen, Z. Peng, J.M. Griffin, L.J. Hardwick, F. Bardé, P. Novák, P.G. Bruce, Reactions in the rechargeable Lithium–O 2 battery with alkyl carbonate electrolytes, J. Am. Chem. Soc. 133 (2011) 8040–8047, http://dx.doi.org/10.1021/ja2021747.
[43] K. Xu, G.V. Zhuang, J.L. Allen, U. Lee, S.S. Zhang, P.N. Ross, T.R. Jow, Syntheses and characterization of lithium alkyl mono- and dicarbonates as components of surface films in Li-Ion batteries, J. Phys. Chem. B 110 (2006) 7708–7719, http://dx.doi.org/10.1021/jp0601522.
[44] L. Gireaud, S. Grugeon, S. Laruelle, S. Pilard, J.-M. Tarascon, Identification of Li battery electrolyte degradation products through direct synthesis and characterization of alkyl carbonate salts, J. Electrochem. Soc. 152 (2005) A850, http://dx.doi.org/10.1149/1.1872673.
[45] D. Aurbach, Y. Gofer, M. Ben-Zion, P. Aped, The behaviour of lithium electrodes in propylene and ethylene carbonate: Te major factors that influence Li cycling efficiency, J. Electroanal. Chem. 339 (1992) 451–471.
[46] S. Tsubouchi, Y. Domi, T. Doi, M. Ochida, H. Nakagawa, T. Yamanaka, T. Abe, Z. Ogumi, Spectroscopic characterization of surface films formed on edge plane graphite in ethylene carbonate-based electrolytes containing film-forming additives, J. Electrochem. Soc. 159 (2012) A1786–A1790.
[47] L. El Ouatani, R. Dedryvère, C. Siret, P. Biensan, S. Reynaud, P. Iratçabal, D. Gonbeau, The effect of vinylene carbonate additive on surface film formation on both electrodes in Li-Ion batteries, J. Electrochem. Soc. 156 (2009) A103, http://dx.doi.org/10.1149/1.3029674.
[48] H. Ota, Y. Sakata, A. Inoue, S. Yamaguchi, Analysis of vinylene carbonate derived SEI layers on graphite anode, J. Electrochem. Soc. 151 (2004) A1659, http://dx.doi.org/10.1149/1.1785795.
[49] H. Nakai, T. Kubota, A. Kita, A. Kawashima, Investigation of the solid electrolyte interphase formed by fluoroethylene carbonate on Si electrodes, J. Electrochem. Soc. 158 (2011) A798–A801.
[50] M. Nie, B.L. Lucht, Role of lithium salt on solid electrolyte interface (SEI) formation and structure in lithium ion batteries, J. Electrochem. Soc. 161 (2014) A1001–A1006.
[51] S.S. Zhang, K. Xu, T.R. Jow, Study of LiBF[sub 4] as an electrolyte salt for a Li-Ion battery, J. Electrochem. Soc. 149 (2002) A586, http://dx.doi.org/10.1149/1.1466857.
[52] K. Xu, S. Zhang, T.R. Jow, W. Xu, C.A. Angell, LiBOB as salt for lithium-ion batteries:a possible solution for high temperature operation, Electrochem. Solid-State Lett. 5 (2002) A26, http://dx.doi.org/10.1149/1.1426042.
[53] K. Xu, S.S. Zhang, U. Lee, J.L. Allen, T.R. Jow, LiBOB: is it an alternative salt for lithium ion chemistry? J. Power Sources 146 (2005) 79–85, http://dx.doi.org/10.1016/j.jpowsour.2005.03.153.
[54] S. Shui Zhang, An unique lithium salt for the improved electrolyte of Li-ion battery, Electrochem. Commun. 8 (2006) 1423–1428, http://dx.doi.org/10.1016/j.elecom.2006.06.016.
[55] M. Dahbi, F. Ghamouss, F. Tran-Van, D. Lemordant, M. Anouti, Comparative study of EC/DMC LiTFSI and LiPF6 electrolytes for electrochemical storage, J. Power Sources 196 (2011) 9743–9750, http://dx.doi.org/10.1016/j.jpowsour.2011.07.071.
[56] H.-B. Han, S.-S. Zhou, D.-J. Zhang, S.-W. Feng, L.-F. Li, K. Liu, W.-F. Feng, J. Nie, H. Li, X.-J. Huang, Lithium bis(fluorosulfonyl)imide (LiFSI) as conducting salt for nonaqueous liquid electrolytes for lithium-ion batteries: physicochemical and electrochemical properties, J. Power Sources 196 (2011) 3623–3632, http://dx.doi.org/10.1016/j.jpowsour.2010.12.040.
[57] G.G. Eshetu, T. Diemant, S. Grugeon, R.J. Behm, S. Laruelle, M. Armand, S. Passerini, In-depth interfacial chemistry and reactivity focused investigation of lithium–imide- and lithium–imidazole-based electrolytes, ACS Appl. Mater. Interfaces 8 (2016) 16087–16100, http://dx.doi.org/10.1021/acsami.6b04406.
[58] J. Braithwaite, G. Nagasubramanian, A. Gonzales, S. Lucero, W. Cieslak, Corrosion of Current-collector Materials in Li-ion Cells, Sandia National Labs, Albuquerque, NM (United States), 1996. http://www.osti.gov/scitech/biblio/414319.
[59] K. Park, S. Yu, C. Lee, H. Lee, Comparative study on lithium borates as corrosion inhibitors of aluminum current collector in lithium bis(fluorosulfonyl)imide electrolytes, J. Power Sources 296 (2015) 197–203, http://dx.doi.org/10.1016/j.jpowsour.2015.07.052.